



**HAL**  
open science

## **GaAs/AlOx high-contrast grating mirrors for mid-infrared VCSELs**

Guilhem Almuneau, Youness Laaroussi, Christyves Chevallier, Frédéric Genty, Nicolas Fressengeas, Laurent Cerutti, Olivier Gauthier-Lafaye

► **To cite this version:**

Guilhem Almuneau, Youness Laaroussi, Christyves Chevallier, Frédéric Genty, Nicolas Fressengeas, et al.. GaAs/AlOx high-contrast grating mirrors for mid-infrared VCSELs. Photonics West, SPIE, Feb 2015, San Francisco, United States. pp.93720S-93720S-9, 10.1117/12.2084515 . hal-01132804

**HAL Id: hal-01132804**

**<https://hal.science/hal-01132804>**

Submitted on 17 Apr 2020

**HAL** is a multi-disciplinary open access archive for the deposit and dissemination of scientific research documents, whether they are published or not. The documents may come from teaching and research institutions in France or abroad, or from public or private research centers.

L'archive ouverte pluridisciplinaire **HAL**, est destinée au dépôt et à la diffusion de documents scientifiques de niveau recherche, publiés ou non, émanant des établissements d'enseignement et de recherche français ou étrangers, des laboratoires publics ou privés.

# GaAs/AlOx high-contrast grating mirrors for mid-infrared VCSELs

G. Almuneau<sup>a,b,\*</sup>, Y. Laaroussi<sup>a,b</sup>, C. Chevallier<sup>c</sup>, F. Genty<sup>c</sup>, N. Fressengeas<sup>c</sup>, L. Cerutti<sup>d</sup>,  
O. Gauthier-Lafaye<sup>a,b</sup>

<sup>a</sup>CNRS, LAAS, 7 avenue du colonel Roche, F-31400 Toulouse, France;

<sup>b</sup>Univ de Toulouse, UPS, LAAS, F-31450 Toulouse, France;

<sup>c</sup>LMOPS, EA n°4423 Université de Lorraine et Supélec, 2 rue Edouard Belin, 57070 Metz, France

<sup>d</sup>Université Montpellier 2; IES; UMR 5214 CNRS; Place Eugène Bataillon, F-34095, Montpellier Cedex 5, France

\*almuneau@laas.fr

## ABSTRACT

Mid-infrared Vertical cavity surface emitting lasers (MIR-VCSEL) are very attractive compact sources for spectroscopic measurements above 2  $\mu\text{m}$ , relevant for molecules sensing in various application domains. A long-standing issue for long wavelength VCSEL is the large structure thickness affecting the laser properties, added for the MIR to the tricky technological implementation of the antimonide alloys system. In this paper, we propose a new geometry for MIR-VCSEL including both a lateral confinement by an oxide aperture, and a high-contrast sub-wavelength grating mirror (HCG mirror) formed by the high contrast combination AlOx/GaAs in place of GaSb/AlAsSb top Bragg reflector. In addition to drastically simplifying the vertical stack, HCG mirror allows to control through its design the beam properties. The robust design of the HCG has been ensured by an original method of optimization based on particle swarm optimization algorithm combined with an anti-optimization one, thus allowing large error tolerance for the nano-fabrication. Oxide-based electro-optical confinement has been adapted to mid-infrared lasers, by using a metamorphic approach with (Al)GaAs layer directly epitaxially grown on the GaSb-based VCSEL bottom structure. This approach combines the advantages of the well-controlled oxidation of AlAs layer and the efficient gain media of Sb-based for mid-infrared emission. We finally present the results obtained on electrically pumped mid-IR-VCSELs structures, for which we included oxide aperturing for lateral confinement and HCG as high reflectivity output mirrors, both based on AlxOy/GaAs heterostructures.

**Keywords:** Vertical Cavity Surface Emitting Laser, oxide confinement, subwavelength diffractive mirror, high contrast gratings, mid-infrared applications

## INTRODUCTION

VCSEL structures emitting in the mid-IR would allow spectroscopic measurements of polluting gas which exhibit strong absorption lines between 2 and 3  $\mu\text{m}$ . The fabrication of such structures is a challenge today and VCSEL emission is still limited at 2.6  $\mu\text{m}$  [1,2]. The use of a high contrast grating (HCG) which can exhibit equivalent Bragg mirror optical properties for a thickness lower than 2  $\mu\text{m}$  [3] should increase electrical, thermal and optical properties. Moreover this type of mirror provides polarization selectivity between TM and TE modes and should improve the stability of the emitted beam.

## HIGH CONTRAST GRATING MIRRORS FOR THE MID-INFRA-RED

Diffractive elements operating in the near- or sub-wavelength regime opens a wide panel of optical functionalities, since in this diffraction regime, both the amplitude and phase of the reflectivity/transmission can be modulated with extraordinary dynamical range[4]. The properties of such high contrast gratings (HCG)

have started to be employed for VCSEL applications, in particular as a new mirror solution in substitution to conventional Bragg mirrors. Thanks to the high flexibility in the design of the optical characteristics of these HCG, the integration of these diffractive elements in the VCSEL structure enables to shape the optical properties of the output beam just by adjusting the geometrical parameters of the gratings. In particular, for VCSELS, the endemic issues of transverse mode and polarization stability can be solved without limitation on the emitted power. Here we propose to integrate a sub-wavelength grating mirror within a Sb-based VCSEL structure emitting in the MIR spectral range. In addition to solve the problems related to the laser structure thickness, such a mirror would allow to control through its design the polarization of the emitted light while contributing to sustainable transverse single-mode operation. Moreover, to ensure sustainable performances of the HCG-VCSEL, with respect for example to technological deviations from the designed geometries, we have implemented an original numerical method based on a robust design of this mirror. This process consists in a numerical optimization of such optical elements based on particle swarm optimization algorithm combined with an anti-optimization one [5]. Finally, the fabrication constraints could then be partially relaxed, in particular for the critical step of the grating reactive ion etching.

### 1.1 HCG Design

Several designs have been optimized with different technological constraints and through a study of the tolerance of the different grating parameters with respect to the error of fabrication; a robust design has been selected for fabrication, and it is obtained from optimization numerical methods with rigorous coupled wave analysis (RCWA) formalism [6,7,8]. Constraints on the optical performances have been fixed to have bottom reflectivity (with an incident light from the substrate) higher than 99.5% for the TM reflectivity while keeping the TE below 90%, and a maximum spectral extension of the high reflectivity stopband.

The typical structure of the high contrast grating developed in this study is presented in Fig. 1, and is composed by a low index layer formed by a buried  $\text{Al}_x\text{O}_y$  layer ( $n=1.66$ ) of thickness  $T_A$ , a plain GaAs layer ( $n=3.3$ ) with a thickness of  $T_L$ , and the grating based on GaAs/air stripes with a thickness of  $T_g$ .

This HCG vertical structure is advantageous for device applications since it is fully monolithic. Moreover, the fabrication flow is based on mature technologies such as dry etching and wet thermal oxidation which are already employed for VCSEL manufacturing in a industrial scale.

With regards to other approaches for HCG based on free standing semiconductor grating membranes, the Al<sub>x</sub>O<sub>y</sub>/GaAs HCG structure presents much better mechanical and thermal properties in the frame on its integration with laser electrically pumped device, and in particular VCSELS.

The etching of the grating slab is the most critical step in the fabrication process flow, thus minimum tolerance values of  $\Delta T_g = \pm 20$  nm and  $\Delta FF = \pm 0.02$  have been fixed to reduce the etching imperfections that might degrade the mirror performances. The tolerance requirements of the grating period  $\Delta \Lambda$  and the GaAs thickness  $\Delta T_L$  have been fixed to 3 nm and 1 nm respectively, based on the e-beam nanolithography accuracy.

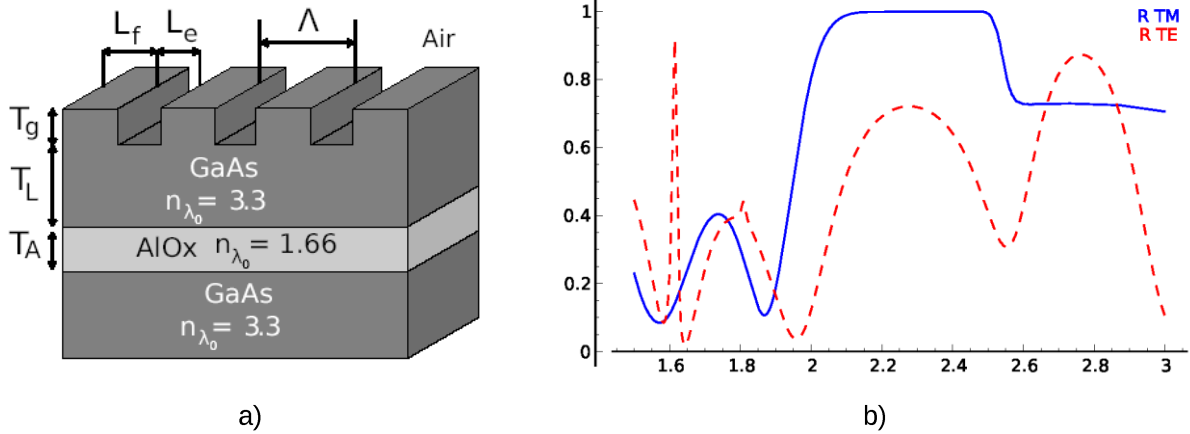


Figure 1: (a) Scheme of the HCG optimized for  $\lambda_0 = 2.3 \mu\text{m}$  exhibiting with  $L_e = 591 \text{ nm}$ ,  $L_f = 554 \text{ nm}$ ,  $T_L = 249 \text{ nm}$  and  $T_g = 713 \text{ nm}$ . (b) Reflection spectra for the TM mode of the optimized structure simulated with the RCWA method.

### TECHNOLOGY OF FABRICATION

The fabrication of HCG mirror is carried out using the following steps: a  $\text{SiO}_x$  hard mask is deposited by plasma-enhanced chemical vapor deposition (PECVD), followed by the electron-beam lithography of the grating in PMMA, and finally the ICP-RIE etching of the grating into GaAs is realized. The grating etch profile must be as close as possible as the designed squared crenel in order to avoid deviation from the aimed optical properties. The most important parameter for keeping a broadband high reflectivity is the grating depth, since it fixes the interference conditions between the Bloch modes. In our case, the optimization method described before gives us a range between 682 and 773 nm for the etch depth, to achieve a sufficient reflectivity with maximum tolerance ranges of the HCG parameters.

We have developed ICP-RIE etching recipes in order to obtain nearly vertical sidewalls, based on  $\text{CHF}_3$  for the hard  $\text{SiO}_x$  mask etch, and  $\text{Cl}_2/\text{N}_2/\text{Ar}$  for the GaAs grating layer etch. The Fig. 2a shows the achieved etch profile with these conditions. The GaAs etch rate was kept relatively slow, in order to better control the groove depth, and to minimize the sidewalls roughness as thus the scattering losses. After the etching step, the measured dimensions of the structure are within the computed tolerances with  $\Lambda = 1145 \text{ nm}$ ,  $\text{FF} = 0.48$ ,  $T_L = 245 \text{ nm}$  and  $T_g = 713 \text{ nm}$ .

The next step in the fabrication of GaAs/AlOx HCG structure is the wet thermal oxidation of the the embedded AlAs layer, in order to produce the low index AlOx layer below the grating. This step is realized after the etch step of mesa larger than the grating area, in order to make the sidewalls of the AlAs layer accessible for oxidizing species. The oxidation step is realized under a controlled moisture atmosphere at a pressure of 500mbar and a temperature 420°C, giving a lateral oxidation rate of 220nm/min. Thanks to the near-IR transmission of the GaAs cap; an optical setup was used for the real time observation and monitoring of the lateral oxidation until the total oxidation of the mesa area (Figure 2b). Due to the chemical reaction occurring during the oxidation, and in particular to the conversion of As to arsine by products, the thickness shrinkage of 10% is typically observed after the conversion of the AlAs layer into  $\text{Al}_x\text{O}_y$  amorphous oxide. Despite this volume shrinkage, and this thermal treatment, no delamination was observed in the oxidized layer.

As mentioned before, the key point in the realization of the HCG structure is the grating etch, since small deviation of grating depth from the design values is sufficient to deteriorate reflectivity performances below the required values for lasing operation.

Etching profiles at different etch times are given in Fig. 3, where we observe that not only the etch depth is particularly tricky to control with accuracy below 10 nm, but also because of the modification of the etch profile within the GaAs material due to the lateral erosion of the hard mask. Thus, a better control and reproducibility of the etch of the grating can be achieved by in-situ reflectometry measurement such as shown on Fig. 4, where at the reflectivity of a 670 nm laser spotted on the grating area has been measured as the function of

the etch depth. In fig 4b, we have obtained by RCWA calculation similar reflectivity oscillation when the grating depth is changed.

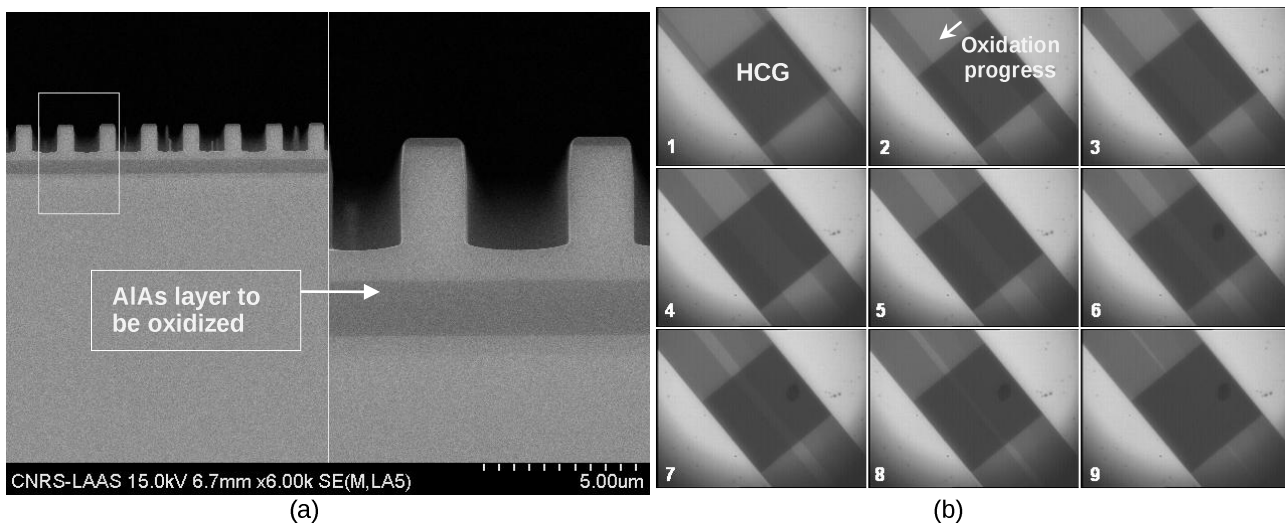


Figure 2 : (a) Scanning Electron Microscopy cross-section image of the grating with the remaining  $\text{SiO}_x$  hard mask at topmost. (b) : Microscopic image of the top view mesa lateral oxidation

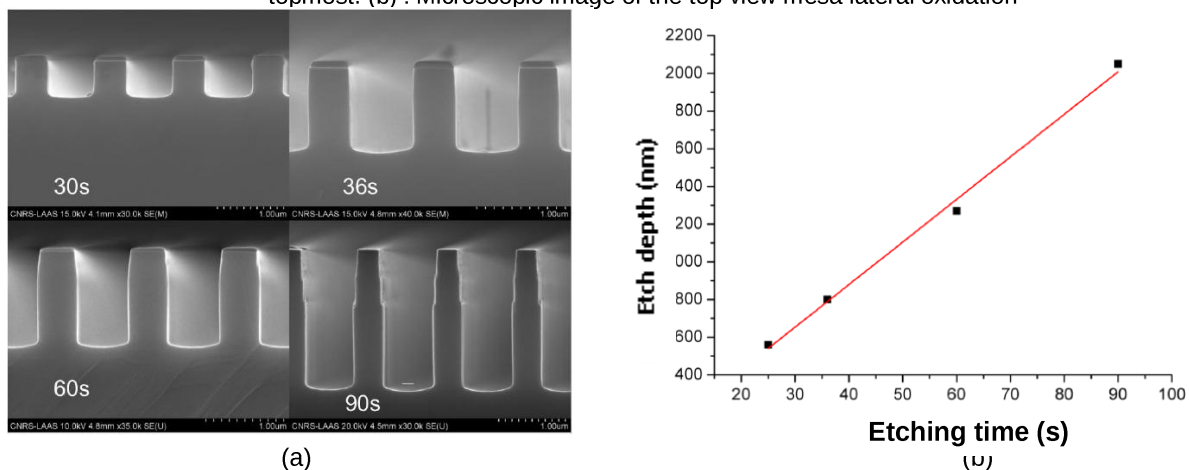


Figure 3 : (a) GaAs grating profile evolution for different etching times. (b) : Linear temporal evolution of the etch depth vs time

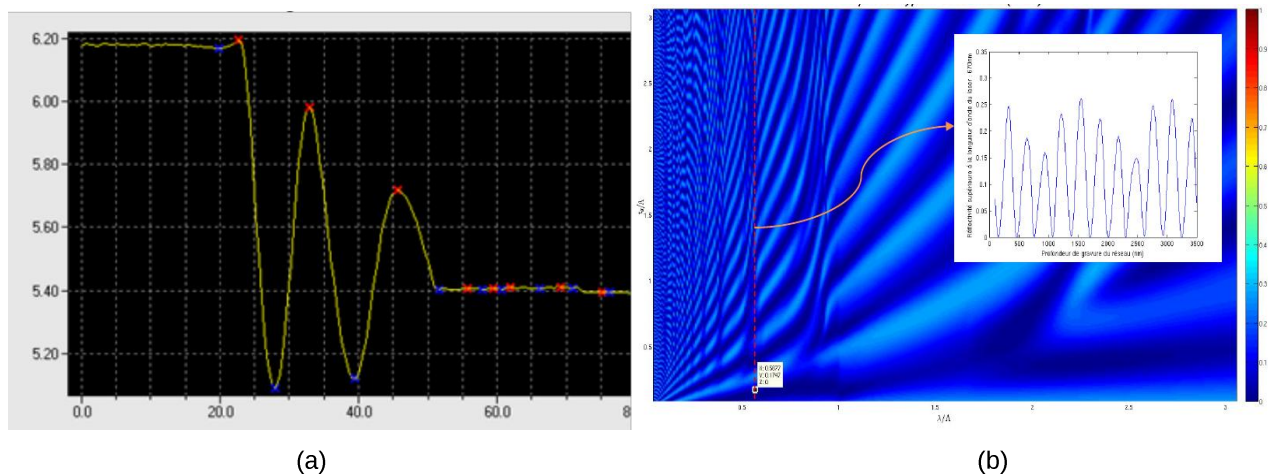


Figure 4 : (a) Laser reflectometry monitoring ( $\lambda=670$  nm) during the ICP-RIE etch of GaAs grating. (b) RCWA simulation of top reflectivity against wavelength and grating depth.

## DESIGN AND FABRICATION OF MID-IR HCG VCSEL

### 1.2 Oxide-based lateral confinement in MIR-VCSELS

The wavelength coverage of VCSELS beyond 2  $\mu\text{m}$ , has been to date limited because of the lack of an efficient lateral confinement method compatible with the employed GaSb and InP material systems [9]. The demonstrations of laterally-confined MIR-VCSEL were obtained either with buried tunnel junctions [10] or using a monolithic VCSEL with selective lateral etching [11]. These confinement methods have enable to improve the electrical and optical properties of the fabricated devices, but the main drawbacks of these approaches is whether the requirement of an epitaxial regrowth, whether a detrimental air gap suspended structure for good mechanical and thermal properties.

We have developed and compared two different new ways for achieving efficient and simple confinement schemes, by employing similarly as for the AlGaAs platform, monolithically integrated oxide-based aperture confinements.

The first approach consists in the selective oxidation of AlAsSb alloys which brings the benefit to be lattice matched on GaSb [12]. Nevertheless, the high antimony composition of these alloys makes its wet oxidation more complex and problematic due to the low volatility of antimony based by-products.

In order to improve the insulator properties of the resulting oxide, we have proposed a two-step process to oxidize buried layers of AlAsSb laterally through thermal wet oxidation at low temperature, followed by a dry thermal annealing to sublimate antimony by-products that remain captive in the oxidized layer. The second phase, which is realized by higher-temperature annealing, significantly improves the insulating properties of the oxidized layer, making it suitable for potential use as a confinement layer in mid-IR laser devices.

The second approach that we have studied and implemented is based on the metamorphic epitaxial growth of AlGaAs directly on GaSb-platform [13]. Then we have demonstrated a novel oxide-confined MIR VCSEL exploiting metamorphic growth and selective thermal oxidation of an Al(Ga)As heterostructure on top of a GaSb-based half-VCSEL structure, and the use of a dielectric output top Distributed Bragg reflector (DBR).

This technology allows the advantages of aluminum arsenide oxidation, a mature and controlled process, to be deployed with other materials systems such as the antimonides for mid-infrared applications.

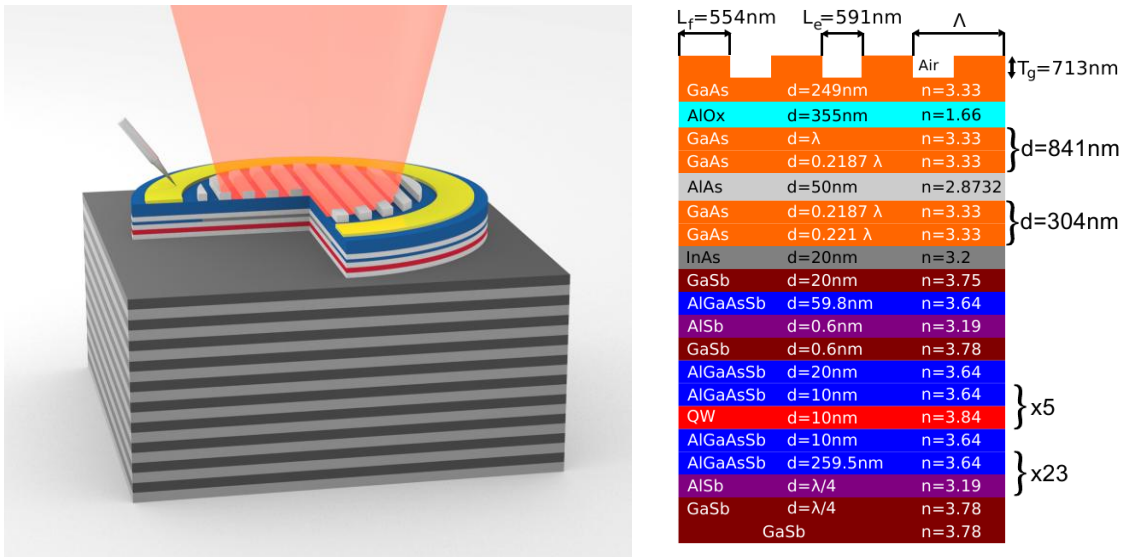


Figure 5. Schematic and vertical structure of the studied oxide-confined HCG MIR VCSEL.

### 1.3 Fabrication

The fabrication process of the HCG-VCSEL is very similar to the one of a standard oxide-aperture VCSEL. The overall process flow consists of realizing the mirror grating etch as described before, then top ring and substrate backside metallizations are applied. Mesas surrounding the HCG are subsequently formed by ICP-RIE, followed by the simultaneous selective lateral thermal oxidation of both  $\text{Al}_{0.98}\text{GaAs}$  layers: one layer forming the low index layer beneath the grating which is completely oxidized, and a lower one to form the oxide aperture as lateral confinement. The final structure is depicted in figure 5.

Once the top grating is etched following the process described before, a resist mask is deposited to protect the grating surface and to define a broader mesa, in order to open lateral access for the oxidation of the AIAs layer beneath the grating (Step 3 on Fig. 6). Afterwards a metallization is realized for the top contact, followed a second mesa etch is done for enabling the lateral oxidation of the second thin AIAs for achieving electrical confinement in the VCSEL device (Step 5 on Fig. 6).

The simultaneous oxidation of both the low index layer of the CHG and the layer providing lateral confinement is then led (Step 6 on Fig. 6). Considering the slower oxidation rate of the 50 nm AIAs confinement layer compared to the upper one within the HCG (400nm), the confinement aperture size can be monitored and controlled, while the HCG  $\text{AlOx}$  layer has been totally oxidized.

For an oxidation process led at  $400^\circ\text{C}$ , the upper and thicker AIAs is oxidized after 60 min, and additionally the oxidation is pursued until 102min for the achieving the desired oxide aperture for the lower  $\text{AlOx}$  confinement layer.

The last step of the HCG-VCSEL process flow consist of a PECVD deposited  $\text{SiOx}$  passivating layer, and the metallization for extending the contact pads. The fig. 7 depicts the final fabricated device.

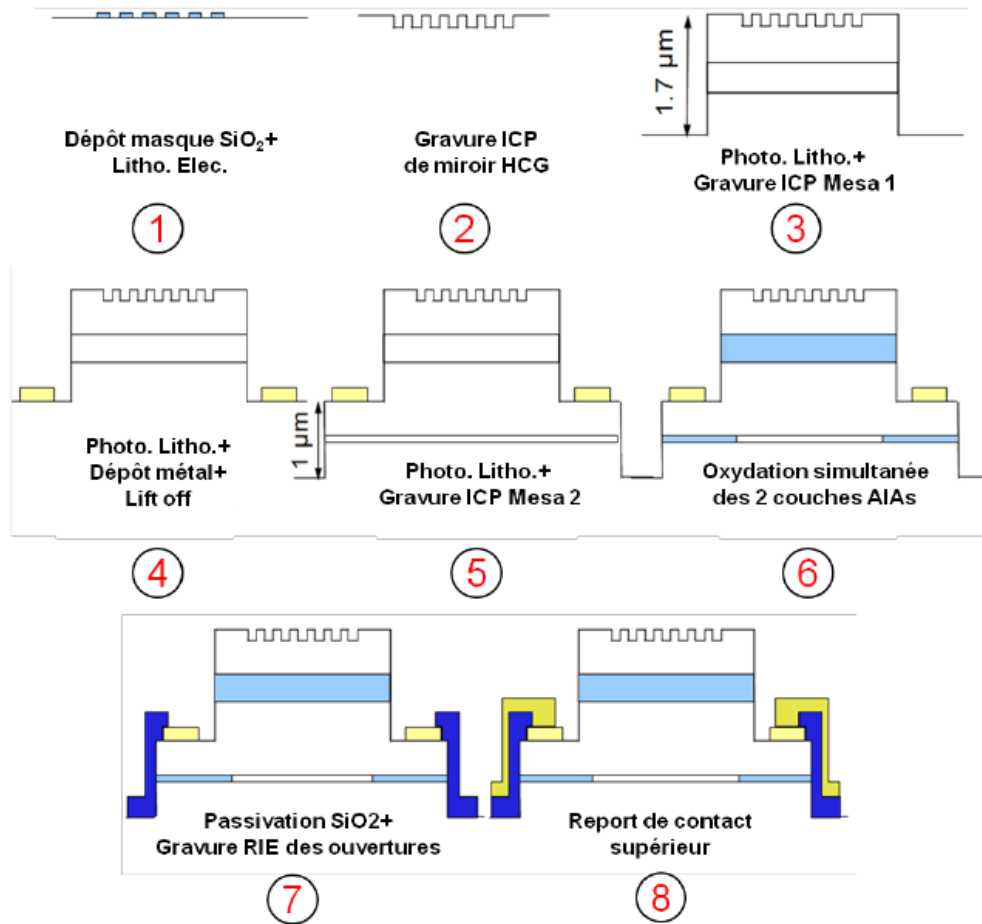


Figure 6 : Process flow of oxide confined HCG MIR VCSEL

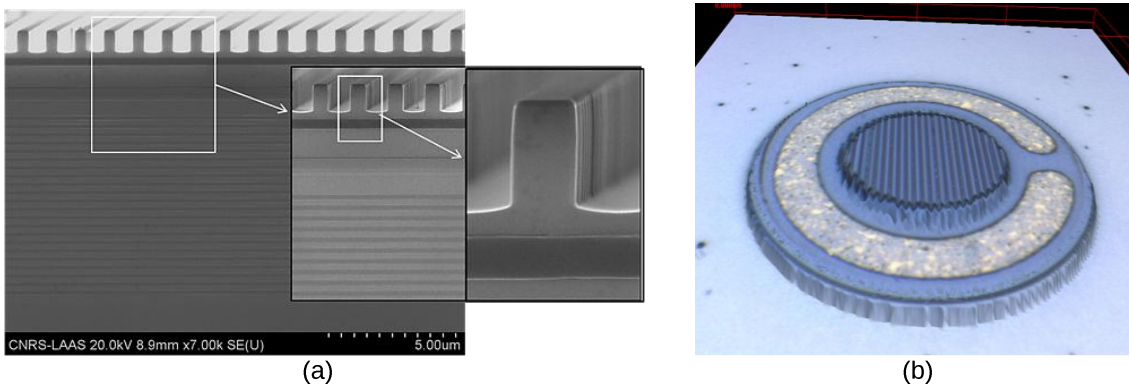


Figure 7: (a) Cross section image by Scanning Electron Microscopy (SEM) of the fabricated HCG-VCSEL after the ICP-RIE processing. (b) Confocal microscope image of the processed HCG-VCSEL

#### 1.4 Results

The VCSEL device has been characterized under electrical pumping at room temperature and in pulsed mode. The VCSEL includes HCG based on GaAs/AlOx material system, grown metamorphically on GaSb



half-VCSEL structure, The gratings lateral size ranges from 19 to 35  $\mu\text{m}$  and lateral confinement is done by oxide apertures ranging from 12 to 28  $\mu\text{m}$ . The voltage-current characteristics show a voltage drop of 0.9V to 3V for an applied current around 5mA as shown on fig. 8a, with increasing voltage drops from large to smaller apertures. This trend agrees with the increase of the series resistance due to current crowding for small aperture sizes.

Despite the good electrical characteristics and the good electroluminescence measured just after the epitaxial growth, we couldn't observe lasing operation on our devices. On Fig. 8b, we present the measured spectrum under pulsed electrical pumping, showing a narrow peak at 2.235  $\mu\text{m}$  related to the resonant cavity effect of the structure. Thus, the fact that no lasing can be achieved proves a lack of reflectivity around 2.25  $\mu\text{m}$  of the HCG mirror, together with a large and unfavorable detuning between the cavity mode and the QW gain centered 2.32  $\mu\text{m}$ . The assumption of low reflective HCG has been confirmed by a cross-section observation with a focus ion beam (FIB) (Fig. 9(a)), revealing substantial deviations of the geometrical parameters of the grating (grating depth, fill factor) from the design. An estimation of the HCG reflectivity with the measured parameters gives a maximum reflectivity around 90%, indeed not sufficient to support lasing operation.

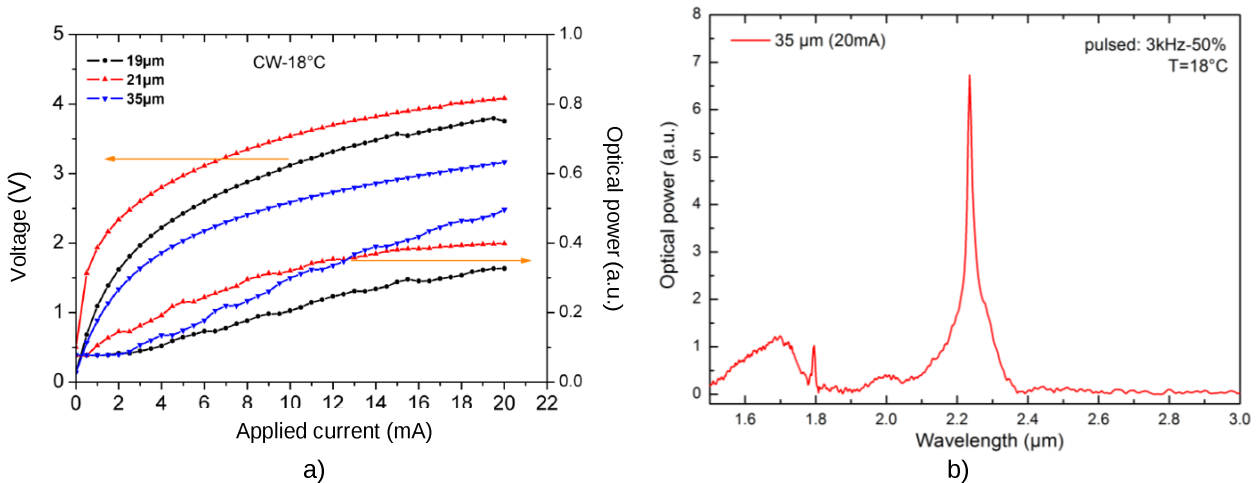


Figure.8 : (a) Top view image by Scanning Electron Microscopy (SEM) of the fabricated HCG-VCSEL after the ICP-RIE processing. (b) Confocal microscope image of the processed HCG-VCSEL

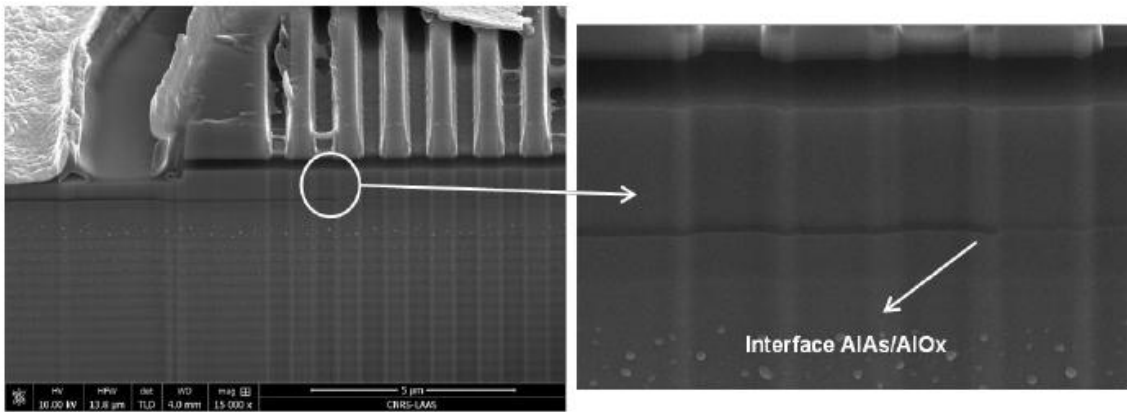


Figure.9 : Focused Ion Beam (FIB) cross-section image of HCG-VCSEL showing the interface Al<sub>0.98</sub>GaAs /AlO<sub>x</sub> of the confinement layer.

## CONCLUSION

As a conclusion, an original VCSEL structure for operation in the mid-IR range has been proposed and fabricated. This mid-IR VCSEL structure combines GaSb-lattice matched epitaxial bottom Bragg mirror and

active region including GaInAsSb-based quantum wells, and a metamorphic GaAs/AlOx HCG structure as top mirror. These technological bricks developed on AlGaAs material system adapted to be use on GaSb platform, enable to realize mid-infrared VCSEL with potentially improved performances and the ability to shape through the design of the grating the output beam properties. We present in this work, the design and fabrication of HCG mirrors with optimized properties while allowing a wide tolerance on geometrical parameter, enabling acceptable margins for the errors during the fabrication process. Finally, we show the first demonstration of electrical pumping and light emission at room temperature on this innovating VCSEL structure.

## ACKNOWLEDGEMENTS

This work was supported by the French National Research Agency (ANR), by the program Blanc under the project Marsupilami, Grant NT09-505624. Also, the authors acknowledge the support of RENATECH (the French Network of Major Technology Centres) within the technological platform of LAAS-CNRS.

## REFERENCES

- [1] A. Ducanhez et al. "Mid-infrared GaSb-based EP-VCSEL emitting at 2.63  $\mu\text{m}$ ," *Electron. Lett.*, **45** (5), 265-267 (2009).
- [2] S Arafin et al, "Electrically pumped continuous-wave vertical-cavity surface-emitting lasers at 2.6  $\mu\text{m}$ ," *Appl. Phys. Lett.* **95** (13), (2009).
- [3] C. Chevallier et al., "Optimized sub-wavelength grating mirror design for mid-infrared wavelength range," *Appl. Phys. A- Mater.*, 10.1007/s00339-010-6059-4 (2010).
- [4] Zhou, Ye, et al. "High-index-contrast grating (HCG) and its applications in optoelectronic devices." *Selected Topics in Quantum Electronics, IEEE Journal of* 15.5 1485-1499 (2009)
- [5] Chevallier, C., Genty, F., Fressengeas, N., & Jacquet, J. "Robust Design by Antioptimization for Parameter Tolerant GaAs/AlOx High Contrast Grating Mirror for VCSEL Application". *Journal of Lightwave Technology*, 31(21), 3374-3380 (2013).
- [6] C. Chevallier et al., "Mid-infrared sub-wavelength grating mirror design: tolerance and influence of technological constraints," *J. Opt.*, 13(2011)
- [7] C. Chevallier et al., «Optimized GaAs High Contrast Grating Design and Fabrication for Mid-infrared Application at 2.3  $\mu\text{m}$ » *Frontiers in Optics 2011*
- [8] M.G. Moharam et al., "Stable implementation of the rigorous coupled-wave analysis for surface-relief gratings: enhanced transmittance matrix approach," *J. Opt. Soc. Am. A*, **12** (5), 1077-1086 (1995).
- [9] A. Ducanhez, L. Cerutti, P. Grech, F. Genty, and E. Tournié, "Mid-infrared GaSb-based EP-VCSEL emitting at 2.63  $\mu\text{m}$ ," *Electron. Lett.* **45**, 265-266 (2009).
- [10] S. Arafin, A. Bachmann, K. Kashani-Shirazi, and M.-C. Amann, "Electrically pumped continuous-wave vertical-cavity surface-emitting lasers at  $\sim 2.6 \mu\text{m}$ ," *Appl. Phys. Lett.* **95**, 131120 (2009).
- [11] Sanchez, D., Cerutti, L. and Tournié, E.: 'Single-Mode monolithic GaSb Vertical-Cavity Surface-Emitting Laser', *Opt. Exp.*, 2012, **20**, (4), pp. 15540-15546
- [12] Laaroussi, Y., Doucet, J. B., Fadel, P., Cerutti, L., Suarez, I., Mlayah, A., & Almuneau, G. "Method for improving the electrical insulating properties of wet thermal oxide of AlAsSb on GaSb substrates". *Applied Physics Letters*, 103(10), 101911 (2013).
- [13] Y. Laaroussi, et al., "Oxide-confined mid-infrared VCSELs," *Electron. Lett.* **48**, 1616-1618 (2012).